ELSEVIER

Polymer 40 (1999) 3069–3082

polymer

Synthesis and characterization of an amine-functional SAN for the compatibilization of PC/ABS blends

G.S. Wildes[a], T. Harada[a], H. Keskkula[a], D.R. Paul[a,*], V. Janarthanan[b], A.R. Padwa[1,b]

[a]Department of Chemical Engineering and Center for Polymer Research, The University of Texas at Austin, Austin, TX 78712, USA
[b]Bayer Corporation, Polymers Division, Springfield, MA 01151, USA

Received 12 January 1998; revised 29 June 1998; accepted 30 June 1998

Abstract

An amine-functional styrene–acrylonitrile (SAN–amine) polymer is proposed as a reactive compatibilizer for bisphenol-A-polycarbonate/acrylonitrile–butadiene–styrene (PC/ABS) blends. This polymer should be miscible with the styrene/acrylonitrile (SAN) copolymer matrix of ABS materials, and the pendant secondary amine groups should react with PC at the carbonate linkage to form a SAN-*g*-PC copolymer. The graft copolymer molecules should reside at the PC/ABS interface and provide improved morphological stability at elevated temperatures by suppressing phase coalescence. This paper describes the synthesis of this reactive compatibilizer and its reaction with carbonate moieties. Characterization of this reaction was done by nuclear magnetic resonance spectroscopy and gel permeation chromatography using model secondary amine and carbonate-containing compounds to facilitate the investigation. The morphology of compatibilized and uncompatibilized PC/SAN blends was examined by transmission electron microscopy. © 1999 Elsevier Science Ltd. All rights reserved.

Keywords: Polymer blend; Reactive compatibilization; Polycarbonate

1. Introduction

Mixtures of bisphenol-A-polycarbonate (PC) with acrylonitrile–butadiene–styrene (ABS) materials represent one of the most important classes of commercial polymer blends [1–10]. Often multiphase blends require some form of compatibilization to obtain useful properties; however, the relatively favorable interaction between PC and the styrene/acrylonitrile copolymer (SAN) matrix of ABS [11–20] apparently makes it possible in this case to produce commercially useful materials without any compatibilizer. Because of this interaction, PC and SAN can be well dispersed in each other and there is good adhesion between the phases [12–14,21–23]. However, blends of PC and SAN (and, thus, ABS) are known to be morphologically unstable and exhibit relatively rapid phase coalescence at elevated temperatures [13,23–28]. Thus, a compatibilization scheme that stabilizes the blend morphology would be useful and perhaps would expand the commercial opportunities for PC/ABS alloys.

This paper outlines a scheme for reactive compatibilization of PC/ABS blends by using a novel SAN with amine functionality. The synthesis and characterization of the SAN–amine compatibilizer, the mechanism of the compatibilizer reactions with polycarbonate, and a demonstration of the effect of this scheme on the morphology of PC/SAN blends are discussed. Subsequent papers will deal with the morphology development and stability of compatibilized PC/ABS blends and the mechanical properties of these materials.

2. Reactive compatibilization scheme

Compatibilization of polymer blends is most effectively accomplished by appropriate block or graft copolymers that locate at the interface between the phase domains in the blend [25,28–35]. These copolymers strengthen the interface, reduce the interfacial tension between the phases and, perhaps most important of all, introduce a steric stabilization mechanism that retards domain coalescence, leading to a finer and more stable phase morphology [23–28,36]. Pre-formed block or graft copolymers can in principle be used for this purpose, but forming the copolymers in situ by chemical reactions during processing has generally proved to be a more useful strategy [2–5,31–35,37–40]. Reactive compatibilization has been most widely practised

---

[*] Corresponding author. Tel.: +1-512-471-5392; Fax: +1-512-471-0542; E-mail: drp@che.utexas.edu

[1] Corresponding author.

PII: S0032-3861(98)00521-7

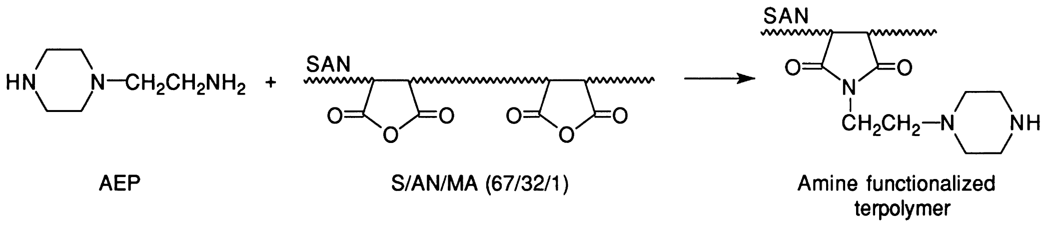

Fig. 1. Schematic of the reaction of S/AN/MA terpolymer with 1-(2-aminoethyl)piperazine (AEP) to form SAN–amine.

for blends involving polyamides by making use of the available amine end groups for reacting with anhydride units in the other phase. The amine–anhydride reaction to form an imide linkage is very rapid at melt-processing temperatures [41–44], and has been widely used and extensively studied in these blend systems for incorporation of polyolefins [45–48] and ABS [49–52]. To a lesser extent, the hydroxyl or carboxyl end groups of polyesters have similarly been used for reactive compatibilization via epoxide, oxazoline, etc. functionality in the other phase [53–56]. Most commercial polycarbonates do not have reactive chain ends since they are generally capped during polymerization to obtain more stable and colorless products [57,58]. As a result, conventional reactive compatibilization schemes are not applicable for polycarbonate-based blends; thus, some new strategy must be devised.

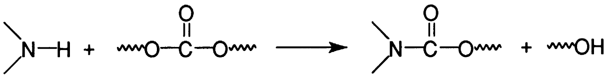

Scheme 1.

After reviewing a number of possible schemes for reactive compatibilization of polycarbonate-based blends, we concluded that the very rapid reaction of amine groups with polycarbonate [59] offered an opportunity worth exploring. Specifically, secondary amines appear to react very predictably and rapidly with carbonate linkages, see Scheme 1. Foldi and Campbell have suggested that this reaction proceeds rather rapidly in solution at room temperature. The reaction of primary amines with carbonate linkages is potentially more complex. The reaction shown in Scheme 1 can be the basis for formation of block or graft copolymers; however, unlike the use of end-group functionality, this route involves chain scission and the formation of a lower-molecular-weight polycarbonate chain with a phenol group at the end. While the latter byproduct may not be desirable, this reaction does provide one of the few available routes to form block or graft copolymers in polycarbonate blends during processing.

To utilize this concept, a way must be devised to incorporate a controlled number of secondary amine groups into a polymer that will be miscible with the SAN phase of ABS materials. To accomplish this, we chose the scheme shown in Fig. 1. An available styrene/acrylonitrile/maleic anhydride (S/AN/MA) terpolymer was selected as the platform to form the amine functional compatibilizer by reactive extrusion with 1-(2-aminoethyl)piperazine (AEP) (see Scheme 2). The rapid reaction of the anhydride unit with the primary amine, [41–44,60] compared with the secondary amine, allows the formation of secondary amine pendant groups as suggested in Fig. 1. Both the original and modified terpolymer should be miscible with SAN copolymers of similar styrene/acrylonitrile ratios.

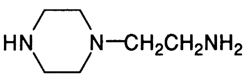

Scheme 2.

The secondary amine group attached to this SAN backbone should then react with polycarbonate to form SAN-*g*-PC copolymer as suggested in Fig. 2. The low maleic anhydride content of the terpolymer should limit the number of pendant secondary amine units, or graft sites, to about five per chain. When added to a PC/ABS blend, it is visualized (see Fig. 3) that the amine-functionalized SAN (SAN–amine) is solubilized in the SAN matrix of the ABS component and reacts with polycarbonate at the PC/SAN interface. The resulting grafted chains subsequently reside at this interface and provide the compatibilizing functions mentioned earlier.

The PC grafts are attached to the SAN backbone by a urethane linkage as shown in Fig. 2. It is known that most polyurethanes are somewhat unstable at processing temperatures above 200°C [59,61–64]. This problem arises because of the dissociation of the urethane linkage shown in Scheme 3, which involves transfer of the labile hydrogen between the nitrogen and oxygen atoms. However, urethanes produced from piperazine or other secondary amines do not undergo this reaction

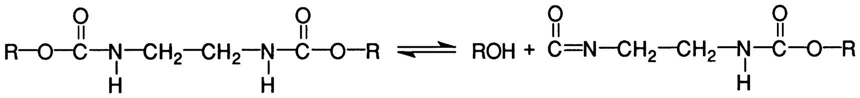

$$R{-}O{-}\overset{O}{\overset{\|}{C}}{-}\underset{H}{\underset{|}{N}}{-}CH_2{-}CH_2{-}\underset{H}{\underset{|}{N}}{-}\overset{O}{\overset{\|}{C}}{-}O{-}R \rightleftharpoons ROH + \overset{O}{\overset{\|}{C}}{=}N{-}CH_2{-}CH_2{-}\underset{H}{\underset{|}{N}}{-}\overset{O}{\overset{\|}{C}}{-}O{-}R$$

Scheme 3.

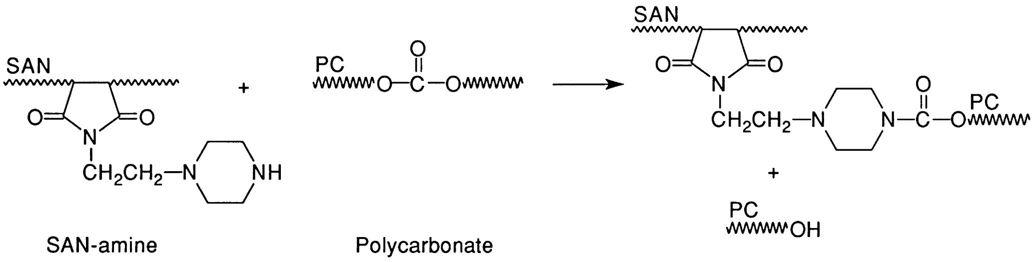

Fig. 2. Schematic of the reaction of SAN-amine with bisphenol-A-polycarbonate to form SAN-*g*-PC.

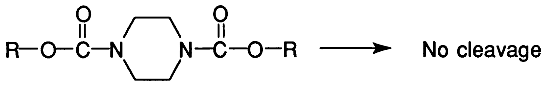

Scheme 4.

(Scheme 4) because there is no labile hydrogen. The literature provides numerous examples showing the improved thermal stability of polyurethanes produced from secondary amines compared with those containing the usual urethane linkage, which contains a labile hydrogen [65–71]. Based on this, it is concluded that the graft linkages shown above should be stable for the times and temperatures involved in melt processing of PC/ABS blends.

3. Experimental

The composition and suppliers of the polymers employed in this work are shown in Table 1. A Brabender torque rheometer with a 50 cm^3 mixing head and standard rotors was used to measure torque as a function of time at 270°C and 60 rev min^{-1} to characterize the melt rheology of the polymers and their blends. Extruded blends were prepared in a Baker–Perkins co-rotating, fully intermeshing twin-screw extruder (15 mm diameter) at 270°C using a screw speed of 160 rev min^{-1}. The polymers were dried in a vacuum oven for at least 12 h at 80°C before melt processing.

Functionalization of the S/AN/MA terpolymer was carried out in a 34 mm (length/diameter ratio = 24) Leistritz co-rotating twin-screw extruder equipped with nine heated barrel sections, a liquid injection port (section 2), vent (zone 7) and die face pelletizer. The barrel and die temperatures were 260°C and 250°C, respectively. The screw operated at 150 rev min^{-1} and pellets were fed at a rate of 20 kg h^{-1}. An excess of liquid AEP, relative to the maleic anhydride content of the terpolymer, was pumped to the reaction zone with a standard HPLC pump equipped with stainless steel tubing. The mole ratio of amine to anhydride was varied as shown in Table 2. The vent stage had a water-cooled vacuum pump system operating at 24 mmHg. Devolatilization has been shown to be a critical step in some reactive processing operations [72]. In this case, devolatilization was required to remove residual AEP and water produced by the imidization. The functionality of the SAN–amine polymer was varied by adding a monofunctional primary amine, 4-(2-aminoethyl)morpholine (AEM) (structure shown in Scheme 5), which competes with AEP for reaction with the maleic anhydride (MA) units in the terpolymer.

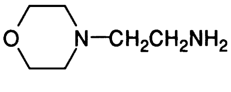

Scheme 5.

Molecular weights of the maleated and aminated terpolymers and polycarbonates were estimated by gel permeation chromatography (g.p.c.). The system uses

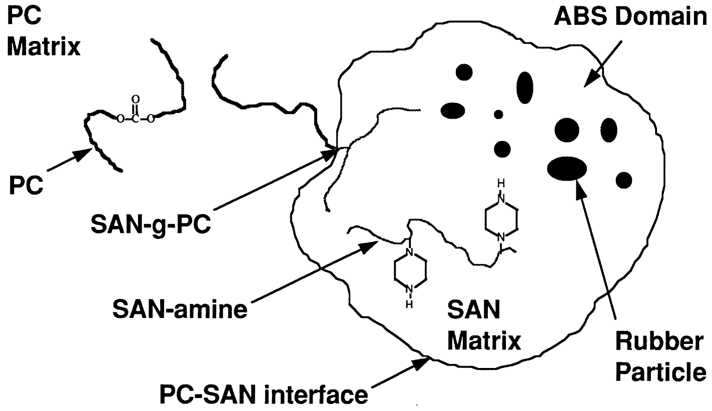

Fig. 3. Schematic of PC/ABS blend compatibilized by graft SAN-*g*-PC copolymers formed from the reaction of SAN–amine with bisphenol-A-polycarbonate during melt processing.

Table 1
Polymers used in this study

Material	Supplier designation	Description/composition	$\bar{M}_n$ (g mol^{-1})	$\bar{M}_w$ (g mol^{-1})	Torque[a] (N m)	Source
VH-PC	Calibre 200-3	Bisphenol-A-polycarbonate Very high molecular weight	13 400	36 000	16.9	Dow Chemical Co.
H-PC	Iupilon E2000	Bisphenol-A-polycarbonate High molecular weight	10 800	32 000	13.1	Mitsubishi Engineering Plastics Corp.
M-PC	Iupilon S3000	Bisphenol-A-polycarbonate Medium molecular weight	8 500	23 700	7.4	Mitsubishi Engineering Plastics Corp.
SAN 25	Tyril 1000	S/AN copolymer 75 wt% styrene 25 wt% acrylonitrile	77 000	152 000	3.4	Dow Chemical Co.
SAN 32.5	Lustran 35	S/AN copolymer 67.5 wt% styrene 32.5 wt% acrylonitrile	59 000	130 000	3.1	Bayer Corp.
S/AN/MA		S/AN/MA terpolymer 67 wt% styrene 32 wt% acrylonitrile 1 wt% maleic anhydride	56 600	119 400	3.9	Bayer Corp.

[a] Brabender torque recorded after 10 min at 270°C and 60 rev min^{-1}.

tetrahydrofuran (THF) as the mobile phase with four American Polymer Standards Corporation AM Gel 5 mm bead columns (a guard column, a mixed column, a column with 500 Å pore size and a column with 100 Å pore size) in series. Analysis was done by a Viscotek Dual Detector Model 250 (viscometry and differential index of refraction detectors) and calibrated with polystyrene standards. Reported molecular weights for the S/AN/MA and SAN–amine are corrected for the acrylonitrile (AN) content of the polymers. There is evidence in the literature that amine functionality can cause polymers to be adsorbed onto the g.p.c. column packing [73,74]. Therefore a small amount of phenyl isocyanate was added to the polymer–THF solution during dissolution. This technique reduces, but may not totally prevent, column adsorption.

The functionalized polymers were examined by photoacoustic Fourier transform infrared spectroscopy (*FT* i.r.) on a Bruker IFS 88 spectrometer equipped with a MTEC photoacoustic accessory at a resolution of 4.0 cm^{-1}. Amine levels were determined by potentiometric titration of the polymer, dissolved in THF, with a standardized solution of perchloric acid in methanol.

Nuclear magnetic resonance (n.m.r.) spectroscopy was done in deuterated chloroform solutions at temperatures of 5, 27 and 50°C on a Varian Inova at 500 MHz. Both ^{13}C and ^{1}H n.m.r. methods were employed for thorough characterization of the reaction of 1-piperonylpiperazine (PIP) with diphenyl carbonate (DPC).

Transmission electron microscopy (TEM) was used to examine the morphology of melt-processed blends of PC/SAN and PC/SAN/SAN–amine. Cryogenically microtomed sections, about 20 nm thick, were prepared on a Reichert–Jung Ultracut E at a sample temperature of −10°C (−45°C knife). The polycarbonate phase of the blends was preferentially stained by exposing the ultra-thin sections to vapor from a 0.5% aqueous solution of RuO_4 at room temperature. TEM imaging was done on a Jeol 200CX microscope operating at 120 keV. Effective particle diameters of the dispersed phase were calculated from the resulting TEM photomicrographs by using NIH Image® digital image-analysis software.

Table 2
Synthesis conditions and characterization of SAN–amine polymers

Sample	AEP/MA (mol/mol)	AEM/MA (mol/mol)	Power (A)	Residual AEP (%)	$\bar{M}_n$ (g mol^{-1})	$\bar{M}_w$ (g mol^{-1})	$\bar{M}_z$ (g mol^{-1})	$\bar{M}_w/\bar{M}_n$	Titer (1)[a]	Titer (2)[a]	Titer (2 − 1)[a]
S/AN/MA	0	0	11	0	56 600	119 400	207 800	2.1	—	0.095	0.095
1	2.00	0	10	0.2	44 500	106 800	189 100	2.4	0.124	0.238	0.114
2	1.50	0	11	nd	45 500	110 200	197 000	2.4	0.110	0.215	0.105
3	1.25	0	11–20	nd	—	—	—	—	—	—	—
4	0.75	0.75	11	nd	47 000	107 800	186 500	2.3	0.166	0.184	0.068

AEP = 1-(2-aminoethyl)piperazine, AEM = 4-(2-aminoethyl)morpholine, MA = maleic anhydride.

[a] Millimoles anhydride/gram of polymer for starting S/AN/MA, millimoles secondary amine/gram of polymer for SAN–amine.

4. Synthesis and characterization of SAN–amine

Secondary-amine-functional SAN polymers were synthesized by derivatization of an S/AN/MA terpolymer with a difunctional amine, 1-(2-aminoethyl)piperazine, as shown in Fig. 1. The reaction of S/AN/MA terpolymer with AEP to form the imide can be carried out in solution by standard imidization methods [75]. These techniques would involve dissolving the cyclic-anhydride-containing polymer in a suitable solvent, reaction with a molar excess of AEP to form the amic-acid intermediate, thermally or chemically mediated dehydration to form the imide and, finally, purification of the polymer to remove solvent and excess AEP. The ability to carry out this entire process by reactive processing would obviate the need for the multiple reaction and purification steps described above.

The anhydride and imide groups were clearly resolved by photoacoustic *FT* i.r. spectroscopy. The disappearance of the strong anhydride band at 1780 cm^{-1} confirmed that no maleic anhydride remained after reaction with AEP. No evidence of carboxylic acid groups was observed before or after reaction with AEP. Concomitant with the synthesis of the desired polymer is the complete removal of any residual AEP. Residual AEP will not only serve to degrade the PC without the formation of compatibilizing graft copolymer, but, as we shall discuss later, leave primary amine groups. Primary amines are efficiently deleterious to PC.

The primary and secondary amines of AEP exhibit different reactivities towards the cyclic anhydride groups of the S/AN/MA. Padwa et al. [41] have shown that the kinetics of reaction of the cyclic anhydride moiety with aliphatic amines is quite sensitive to the molecular structure of the amine with factors of 10 differences in reactivity occurring readily. The molar excess of AEP required to achieve complete conversion of the cyclic anhydride to secondary amine should be governed, to a first approximation, by the differential reactivity of the primary and secondary amine groups of AEP. If the difference in reactivity of the two amine groups towards the cyclic anhydride is sufficiently large, then small molar excesses of AEP, relative to cyclic anhydride, could be used without concomitant branching and crosslinking of the SAN backbone. If this difference is very large, then the molar excess approaches zero. Achieving low molar excesses of AEP facilitates the removal of excess AEP, the presence of which would interfere with the desired reactive compatibilization chemistry.

An S/AN/MA terpolymer containing 32 wt% AN and 0.93 wt% MA was functionalized with different molar excesses of AEP, as shown in Table 2; the composition of the starting terpolymer was characterized as described previously [42]. Sample 1 had a 100% molar excess of AEP charged to the reaction zone of the twin-screw extruder. This amounts to 2.4 wt% of the polymer. The power drawn by the extruder was quite similar to that of the S/AN/MA terpolymer with no added amine. The level of residual AEP, owing to the inability to fully devolatilize the large excess of AEP, was found to be 0.20% by weight by gas chromatography (g.c.). Since free AEP has both secondary and primary amine groups that can react with polycarbonate, this level of residual AEP corresponds to 30% of the reactive secondary amines present in the fully functionalized SAN–amine polymer. As discussed later, minimization of non-bound amine is important to maintain polycarbonate molecular weight during reactive compatibilization. Sample 2 was made with a 50% molar excess of AEP. Once again, the extruder power was quite similar to that of the previous case. For the preparation of sample 3, the amount of AEP was reduced to a 25% molar excess. The extruder power fluctuated in a smooth fashion wherein it would increase for a period of time, about 2 to 5 min, then decrease. This indicates that the extruder conditions were unstable and slight changes in feeding rates of either S/AN/MA or AEP would result in the onset of power increases due to crosslinking. The critical molar excess of AEP to cyclic anhydride for this process is about 25%. As the charged molar excess of AEP decreases, the level of residual AEP decreases to an undetectable level.

Finally, sample 4 was prepared by using a mixture of AEP and 4-(2-aminoethyl)morpholine. AEM was chosen for its structural similarity to AEP. The primary amine groups of these two molecules should exhibit the same reactivity towards the cyclic anhydride. The experiment was carried out at a 50% molar excess of total primary amine. The extruder ran well and in a very stable fashion. The use of a mixture of monofunctional AEM and difunctional AEP allows full control of the pendant amine functionality that can be incorporated into the S/AN/MA terpolymer.

As shown in Table 2, g.p.c. analyses of the polymers show small decreases in the observed molecular weight of the polymer compared with the starting S/AN/MA terpolymer. The aminated terpolymer is highly adsorbed onto the g.p.c. column packing as indicated by large decreases in total detected peak area compared with the starting terpolymer. The addition of a small amount of phenyl isocyanate to cap the amine results in comparable levels of detection for the S/AN/MA and SAN–amine polymers. The conversion of the cyclic anhydride to the isocyanate-capped amine-functional derivative can certainly result in some solution conformational changes of the polymer. The polydispersity index ($\bar{M}_w/\bar{M}_n$) increases from 2.11 to a maximum of 2.42 upon derivatization. Considering that the weight-average molecular weight of the starting terpolymer and the amine derivatives are within 10% of each other, there is very little, if any, branching or crosslinking present. Polymers made with a 25% molar excess of AEP were generally not soluble or showed the presence of significant levels of polymer gels.

To determine the level of bound amine functionality, a solution of the polymer in acetone was titrated potentiometrically with perchloric acid. The titration curve shows two inflection points, the first (Titer 1) associated with the tertiary amine of AEP and the second (Titer 2) resulting from the secondary amine. Table 2 shows the secondary amine titer of the polymer obtained by taking the difference between the endpoints of the secondary and tertiary amines, respectively. The starting polymer contains 0.095 mmol of anhydride per gram of polymer. The titers of the polymers are somewhat greater than the titer of the starting terpolymer, most likely due to the presence of some residual, unbound AEP. The titer of sample 4 is somewhat greater than the expected value of 0.048. The secondary amine content of this polymer is about 65% of the theoretical SAN–amine product. This difference may be due to reactivity differences between AEP and AEM. Clearly, the level of secondary amine functionality can be readily tailored to be any amount from molar equivalence of the cyclic anhydride level of the starting terpolymer to zero. The choice of the specific level of functionality will be governed by the design of the reactive compatibilizer precursor.

5. Polycarbonate reaction with secondary amines

As previously described, SAN-*g*-PC copolymer formation relies on the rapid reaction of the pendant secondary amine with the carbonate linkages in PC, as suggested in Fig. 2. However, with conventional *FT* i.r., n.m.r. and g.p.c., it is difficult to establish what reactions actually occur or to quantify the extent of these reactions owing to the low functional levels of the SAN–amine and often overlapping peaks in macromolecular systems. Therefore, strategies based on low-molecular-weight compounds were used to model the PC/SAN–amine compatibilization chemistry.

5.1. Model reaction scheme

To verify the carbonate–secondary amine reaction suggested by the literature [59], DPC and PIP were selected for model studies by n.m.r. These compounds were mixed in various proportions at about 3 wt% total solids in deuterated chloroform ($CDCl_3$) solution at temperatures of 5, 27 and 50°C and allowed to react for times of 5 min to 4 h. The reaction expected is that shown in Scheme 6. Although the literature on the use of n.m.r. characterization of the formation of such urethane structures is somewhat limited [61,62,76–80], available techniques can clearly distinguish between secondary amine, carbonate and urethane moieties. Typical ^{1}H-n.m.r. spectra for DPC and PIP in $CDCl_3$ are shown in Fig. 4(a) and (b), respectively. These reactants were mixed in $CDCl_3$ at room temperature and then analyzed by n.m.r. The ^{1}H-n.m.r. spectrum for the solution after mixing for 24 h is shown in Fig. 4(c). Complete reaction is confirmed by the disappearance of the secondary amine peak, corresponding to the PIP reactant, at 2 ppm, see Fig. 4(b). The B peak, due to the hydrogen nearest the amine hydrogen, has split and shifted from 2.8 ppm, see Fig. 4(b), to a doublet at 3.6 and 3.7 ppm, see Fig. 4(c). Additionally, the short broad peak near 6 ppm, see Fig. 4(c), confirms the presence of phenol, one of the two expected reaction products shown in Scheme 6.

^{13}C-n.m.r. was also used to characterize the reaction of DPC with PIP. A ^{13}C spectrum of DPC in $CDCl_3$ is shown in Fig. 5(a). The carbonate peak, E, is at 152.01 ppm. After careful examination of the solution spectrum after mixing in $CDCl_3$ for 24 hours, see Fig. 5(b), the 151.11, 153.76 and 156.18 ppm peaks can be assigned. The phenol peak at 156.18 ppm was first identified by adding excess phenol to the post-reaction solution. Proton-coupled ^{13}C-n.m.r. (see Fig. 6) was then used to distinguish the urethane peak, D, at 153.76 ppm (153.77 ppm in Fig. 6) from the peak due to the aromatic carbon bonded to the oxygen adjacent to the urethane, C, at 151.11 ppm (151.10 ppm in Fig. 6). Therefore, from the ^{13}C-n.m.r. analysis, there is evidence of the disappearance of the carbonate peak as well as the appearance of both the phenol and urethane peaks. These results, along with the evidence for disappearance of the amine peak from ^{1}H-n.m.r., confirm the chemical structure of the expected reaction products shown in Scheme 6. No side reaction products were detected.

5.2. Kinetics of DPC/PIP reaction

The kinetics of the reaction of DPC with PIP carried out in $CDCl_3$ solution (3 wt% total solids) at temperatures from 5 to 50°C was also investigated by n.m.r. The results of these experiments are interpreted in terms of the following simple model for a

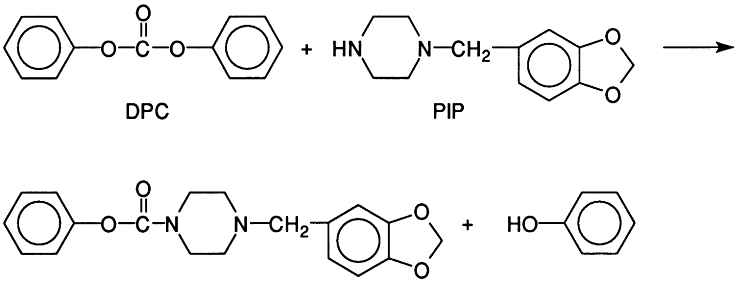

Scheme 6.

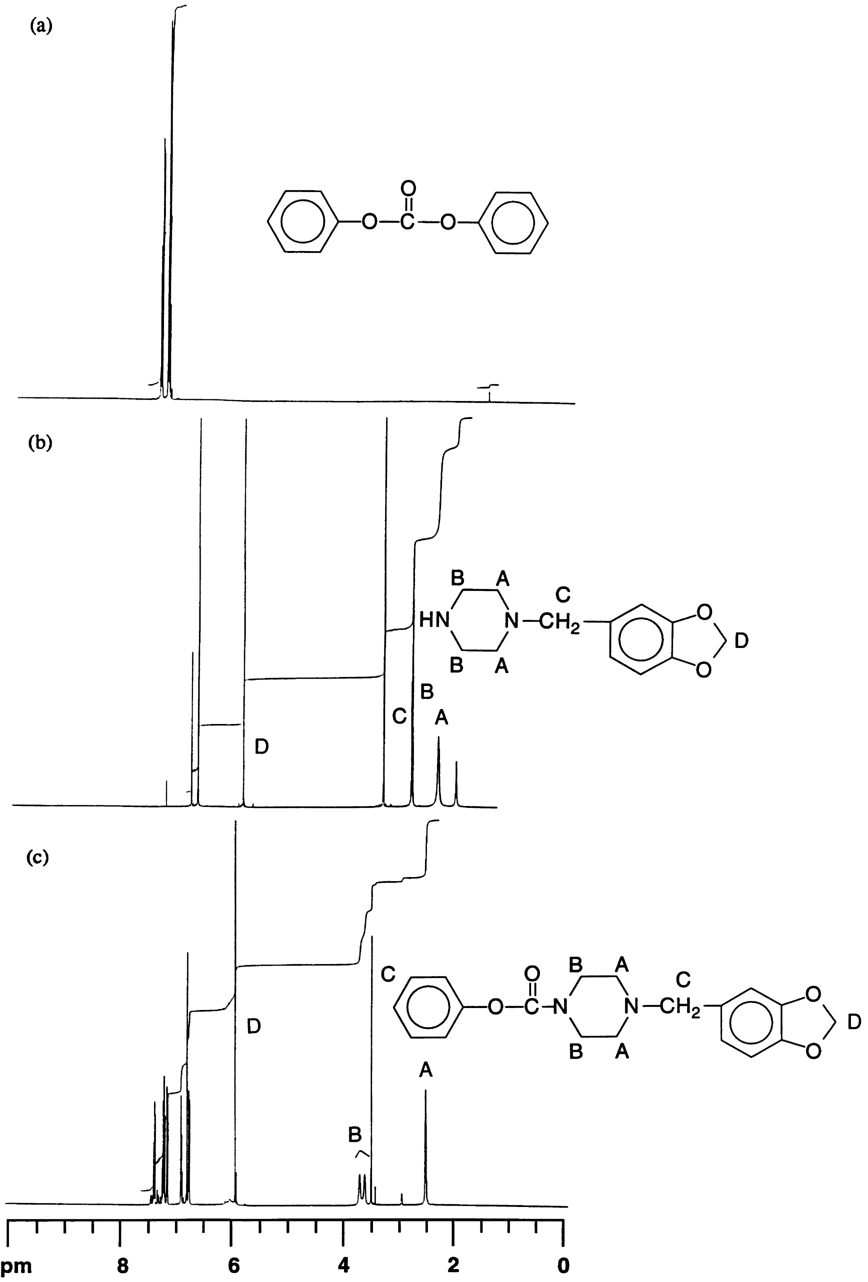

Fig. 4. ^{1}H-n.m.r. spectra of (a) DPC in $CDCl_3$, (b) PIP in $CDCl_3$, and (c) DPC and PIP in $CDCl_3$ (3 wt% total solids) after reaction at room temperature for 24 h.

second-order reaction

$$A + B \longrightarrow \text{products} \tag{1}$$

$$\frac{dx}{dt} = k(a-x)(b-x) \tag{2}$$

where a = initial concentration of A, b = initial concentration of B, and x = molar concentration of reactants that have been consumed at time t. The solution to Eq. (2) with $a \neq b$ for the initial conditions $x = 0$ at $t = 0$ is

$$\ln\frac{b(a-x)}{a(b-x)} = (a-b)kt \tag{3}$$

We take B as the limiting reactant and define $P = x/b$ as the fraction of B reacted. The fraction P can be calculated from the relative heights of the amine and a control peak from the ^{1}H-n.m.r. spectra. By using the measured values of P as a function of time, the second-order reaction rate parameter, k, can be found from the slope of a plot of the data in the form suggested by the following equation

$$\frac{\ln\left[\dfrac{\frac{a}{b}-P}{1-P}\right] + \ln\dfrac{a}{b}}{b\left(\dfrac{a}{b}-1\right)} = kt \tag{4}$$

Fig. 7 shows such plots for different relative concentrations of A (DPC) and B (PIP). In general, the data are described

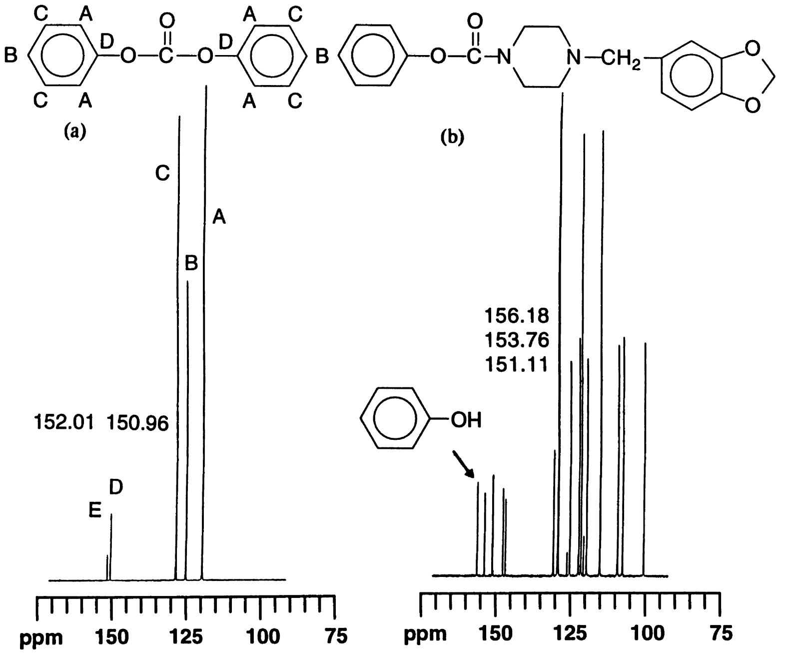

Fig. 5. ^{13}C-n.m.r. spectrum of (a) DPC in $CDCl_3$, and (b) DPC and PIP in $CDCl_3$ (3 wt% total solids, DPC/PIP = 1.0/0.1) after reaction at room temperature for 24 h.

rather well by this simple model. A detailed examination of different experiments shown in Fig. 7 suggests that all ratios of DPC to PIP may not be described by the same straight-line relationship, i.e., same *k*, as expected from this simple model. The case of practical interest to us is the one where there is a very large number of carbonate linkages per secondary amine groups. Of course, loss of experimental accuracy precludes modeling this case using the approach employed to develop the results in Fig. 7. Indeed, experimental errors may be some part of the apparent departure from the model.

Fig. 8 shows the reaction kinetics for DPC with PIP in $CDCl_3$ as a function of temperature for DPC/PIP = 1/0.1. The range of temperatures available for examination was limited by the boiling point of $CDCl_3$. Nevertheless, the reaction rate increases strongly with increasing temperature; however, it is not feasible to extrapolate the kinetics of this reaction to melt-processing temperatures (270°C) because of the narrow temperature range of these measurements. Table 3 summarizes the reaction rate parameters, *k*, obtained from these model experiments.

5.3. Melt reaction of PC with PIP

The model experiments outlined above provide information about the products and kinetics of the carbonate–secondary amine reaction in solution at relatively low temperatures. However, the compatibilization scheme suggested in Fig. 2 must occur in the melt state at temperatures of the order of 270°C. Here, we use additional model experiments that give further information about this reaction scheme and its kinetics under these more stringent

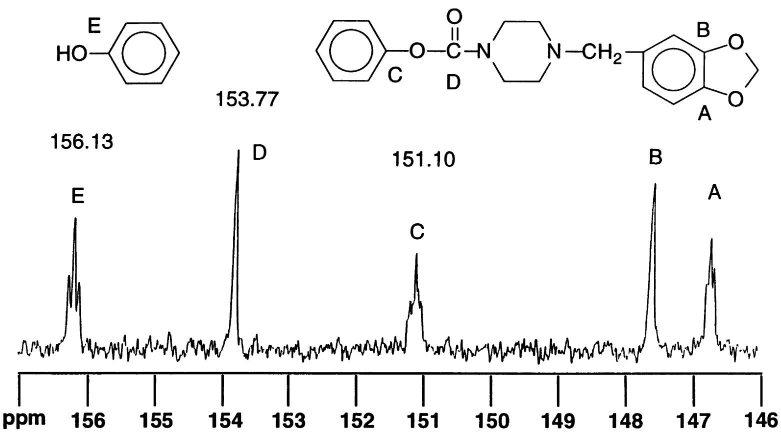

Fig. 6. Proton-coupled ^{13}C-n.m.r. spectrum of DPC and PIP in $CDCl_3$ (3 wt% total solids, DPC/PIP = 1.0/0.1) after reaction at room temperature for 24 h; D is the urethane peak.

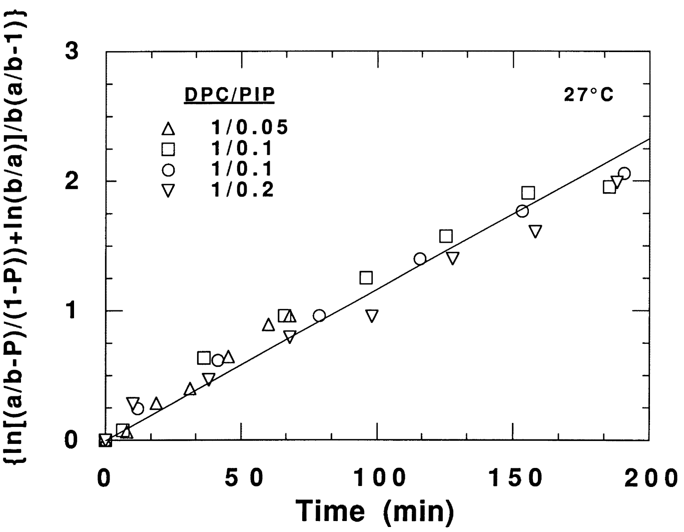

Fig. 7. Kinetic analysis of the reaction of DPC with PIP in $CDCl_3$ at room temperature as a function of DPC/PIP ratio according to the second-order model described in the text; the slope of the lines gives the reaction rate parameter *k*.

conditions, but, of course, the information obtained is less detailed than that described above. The experiment consists of melt mixing of polycarbonate with the model secondary amine compound PIP (selected to have relatively low volatility at these temperatures). On the basis of the results obtained above, we expect that when small amounts of PIP are added to PC that chain scission should occur as shown in Scheme 7, where $x + y + 1 = n$. The original end groups of the polycarbonate, denoted here by E, are not specifically identified for the commercial polycarbonates employed in this work. It is statistically possible, but increasingly unlikely the lower the content of PIP, that two PIP molecules could react with the same PC chain to produce the product shown in Scheme 8. In the case of SAN–amine reaction with PC, multiple reactions of this sort can lead to crosslinked structures or gel, so it is important to limit the amount of amine functionality to the minimum required.

To quantify the reaction of PC with PIP, two types of experiment were performed. Melt rheology studies of polycarbonate, the material designated as H-PC in Table 1, with varying amounts of PIP were conducted in a Brabender batch mixer at 270°C and 60 rev min^{-1}. As can be seen in Fig. 9, the addition of PIP to polycarbonate causes a significant reduction in the viscosity of the melt; the reduction in torque is complete by the time the materials have reached thermal equilibrium, indicating the reaction is complete

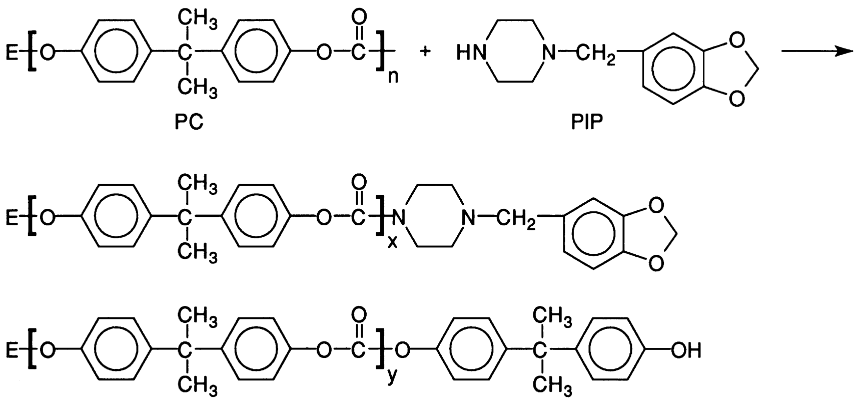

Scheme 7.

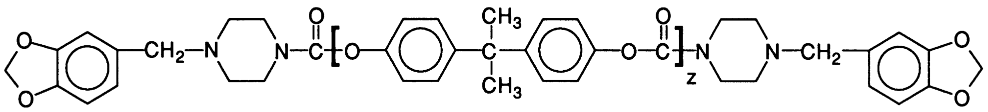

Scheme 8.

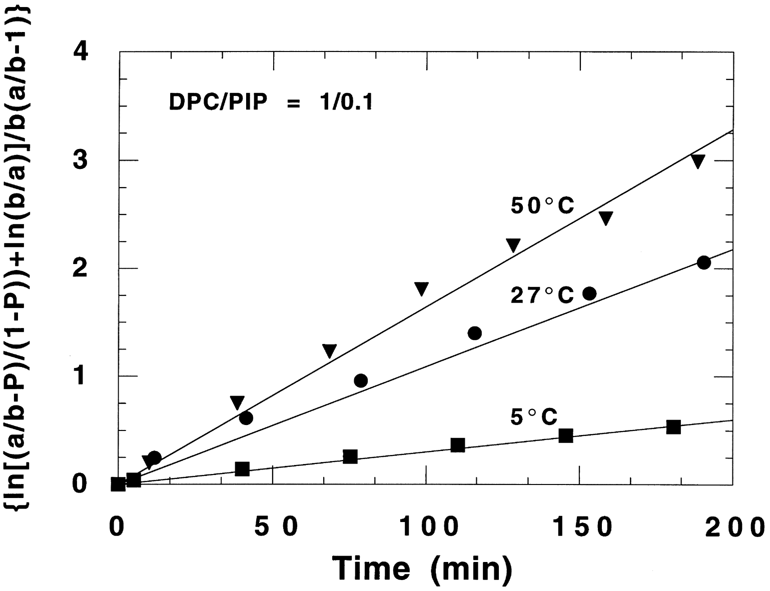

Fig. 8. Effect of temperature on the kinetics of DPC/PIP (1/0.1) mixtures reacted in $CDCl_3$.

within the time frame of melting of the blend constituents. The reduction in viscosity is expected because each PIP molecule should cause scission of one PC chain as suggested by Scheme 7. Based on the kinetics observed for the reaction of DPC with PIP in solution near room temperature (see Fig. 7 and Table 3), the reaction at melt temperatures should be extremely fast. Brabender samples were taken after mixing for 20 min, after which the polycarbonate number-average molecular weight was determined by g.p.c. The results are plotted versus the molar ratio of PIP to PC chains in Fig. 10. Similar data for H-PC and PIP mixtures refluxed for 2 h in boiling THF are also included in this plot. The solid line in Fig. 10 is the calculated molecular weight ratio assuming each amine causes one PC chain scission as suggested by Fig. 10. That is, the line was calculated from the relationship

$$\frac{\bar{M}_n}{(\bar{M}_n)_0} = \frac{1}{1+r} \tag{5}$$

where $(\bar{M}_n)_0$ is the number-average molecular weight of the PC before reaction with PIP and $r =$ moles of PIP/moles of PC chains. The data in Fig. 10 show that the reaction of PC with PIP is quantitative and, 270°C in the Brabender for times sufficient to melt polycarbonate or 65°C in solution for less than 2 h, is a sufficient temperature–time condition to reach the calculated limit of the reaction.

Table 3
Second-order rate coeffcient for reaction of DPC with PIP in $CDCl_3$ (3 wt% total solids)

PIP/DPC ratio	Temperature (°C)	k ($M^{-1}\,s^{-1}$)
1/0.1	5	0.00301
1/0.1	27	0.0112
1/0.1	50	0.0164
1/0.05	27	0.0114
1/0.2	27	0.0109

6. Morphology

The evidence presented above supports the hypothesis that addition of the amine-functionalized SAN material to PC/ABS blends leads to graft copolymer formation during melt processing as proposed in Fig. 2. This in turn should lead to improved control of morphology by some reduction in the interfacial tension between PC and the SAN matrix of ABS, but perhaps more importantly by reducing the frequency of domain coalescence through a steric stabilization mechanism [24,27,28]. This is demonstrated here by comparison of the morphology of blends of PC and SAN (no rubber phase was included to simplify the demonstration) prepared by extrusion with and without an SAN–amine compatibilizer.

Blends of 70% by weight of a medium-molecular-weight polycarbonate, M-PC in Table 1, with 30% SAN32.5 and 24% SAN32.5 plus 6% SAN–amine compatibilizer were melt mixed in a Baker–Perkins co-rotating, fully intermeshing twin-screw extruder (15 mm diameter) at 270°C at a screw speed of 160 rev min^{-1}. Observation of the extrudate showed that 70/30 blends of PC/SAN had very low melt strength. However, compatibilized blends with as little as 1% SAN–amine exhibited improved melt strength over the uncompatibilized blends, which is evidence of chemical grafting and compatibilization between the phases. Samples for morphology analysis by TEM were cut from the center of the pelletized extrudate. The TEM photomicrographs in Fig. 11 show that there is a significant reduction in the average dispersed domain size in the

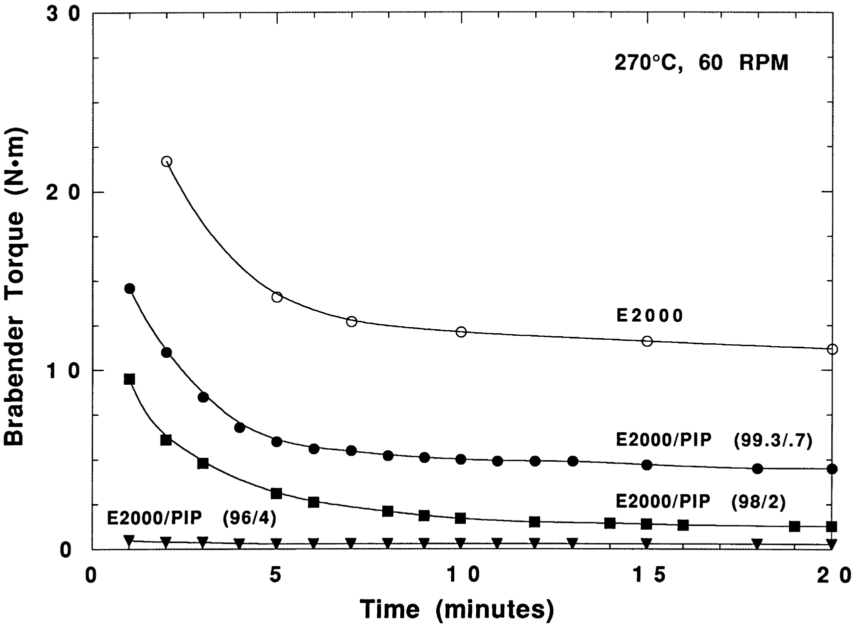

Fig. 9. Brabender torque versus time for mixtures of H-PC with PIP at 270°C and a rotor speed of 60 rev min^{-1}.

compatibilized ($\bar{d}_w = 0.24\,\mu m$) versus uncompatibilized ($\bar{d}_w = 1.19\,\mu m$) blends. Blends of a very-high-molecular-weight polycarbonate, VH-PC in Table 1, with SAN25 in a 70/30 ratio and with SAN25/SAN–amine compatibilizer in a 70/24/6 ratio were mixed at 270°C at a speed of 60 rev min^{-1} in a Brabender mixer for 20 min. Samples weighing approximately 2.5 g were taken from the middle of the melt and quenches in ice water and then analyzed by TEM. The resulting photomicrographs show a reduction in the average dispersed domain size in the compatibilized ($\bar{d}_w = 0.50\,\mu m$) versus uncompatibilized ($\bar{d}_w = 2.16\,\mu m$) blends (see Fig. 12) that is comparable to the decrease seen in the extruded blends. For the present demonstration of this compatibilization scheme, we have chosen these blends to show that particle-size reduction can be effectively accomplished for different shear rates, polycarbonate molecular weights and AN contents of the SAN copolymers. All of these variables (in addition to compatibilization) can have a significant effect on the resulting morphology and are currently being investigated in more detail.

The viscosity of many reactively compatibilized blends increases dramatically with the formation of graft or block copolymer during melt processing [52,81]. Here, the Brabender torque values and the extruder current indicate that the melt viscosities for the compatibilized blends were higher than for the uncompatibilized blends by about 25–50% (see Fig. 13); however, this increase is less than that seen in many compatibilized blend systems. This observation is attributed to the competing effects of grafting and chain scission which produce SAN-*g*-PC chains with lower-molecular-weight PC chains as a byproduct.

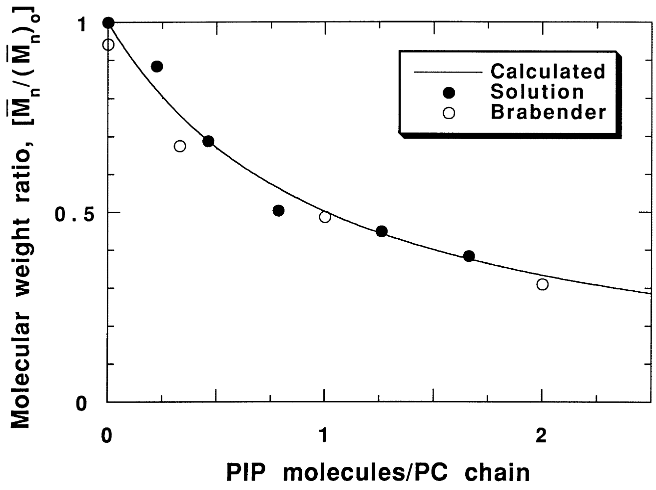

Fig. 10. Molecular-weight reduction of polycarbonate as a function of the mole ratio of PIP/PC chains for melt and solution reaction. The solid line was calculated from Eq. (5).

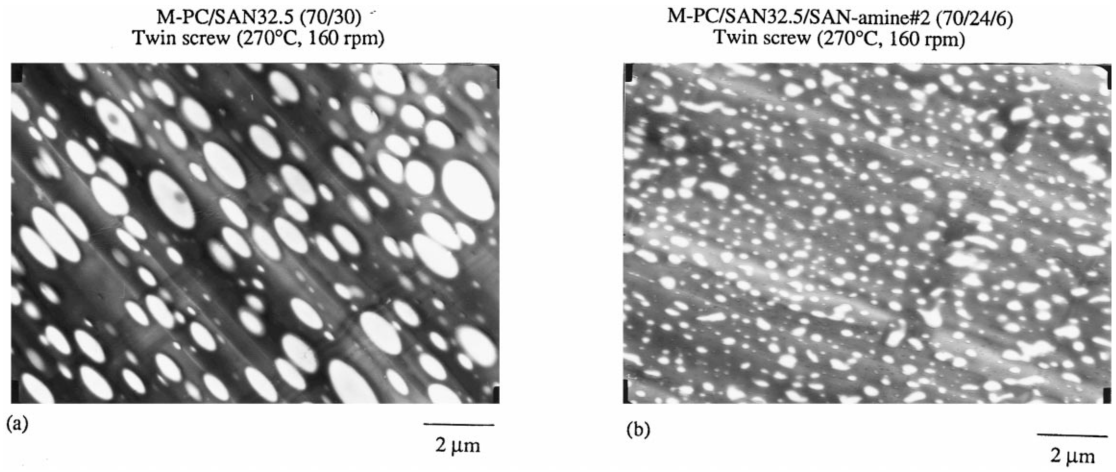

Fig. 11. TEM photomicrographs for extruded blends (twin screw at 270°C at a screw speed of 160 rev min^{-1}) stained with RuO_4: (a) M-PC/SAN32.5 (70/30) ($\bar{d}_w = 1.19\ \mu m$), (b) M-PC/SAN32.5/SAN–amine#2 (70/24/6) ($\bar{d}_w = 0.24\ \mu m$).

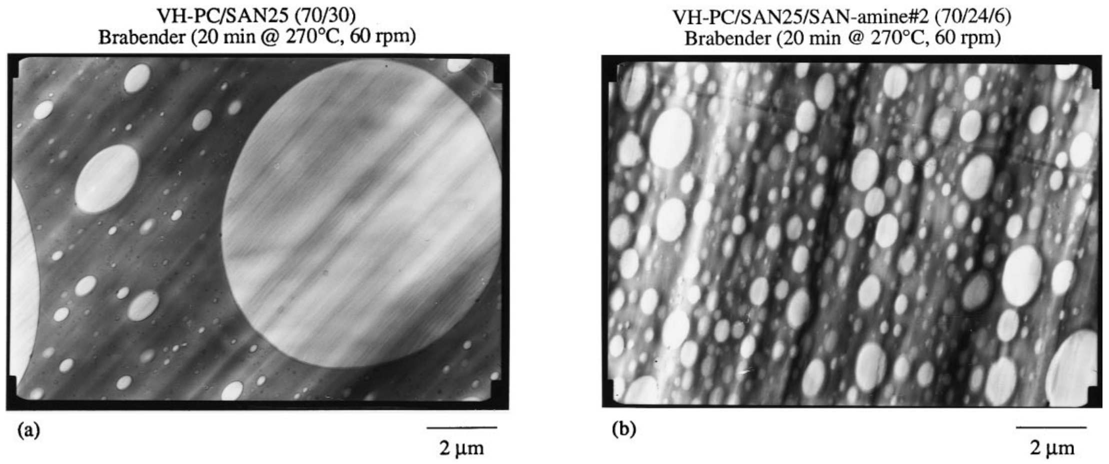

Fig. 12. TEM photomicrographs for Brabender-mixed blends (270°C at a rotor speed of 60 rev min^{-1}) stained with RuO_4: (a) VH-PC/SAN25 (70/30) ($\bar{d}_w = 2.16\ \mu m$), (b) VH-PC/SAN25/SAN–amine#2 (70/24/6) ($\bar{d}_w = 0.50\ \mu m$).

7. Conclusions

A scheme proposed for the reactive compatibilization of PC/ABS blends has been evaluated. The compatibilization uses a novel secondary amine functional SAN (SAN–amine) which appears to react predictably, rapidly and quantitatively with the carbonate linkages in bisphenol-A-polycarbonate to form SAN-*g*-PC copolymer. The SAN–amine compatibilizer was formed by reaction of an S/AN/MA terpolymer with 1-(2-aminoethyl)piperazine (AEP). *FT*i.r. and titration techniques were used to confirm the complete loss of maleic anhydride functionality in the SAN–amine and that all pendant amines are secondary. N.m.r. characterization confirmed the disappearance of both amine and carbonate functionalities as well as the appearance of urethane and phenol peaks during reaction of a diphenyl carbonate with a model secondary amine compound in solution at room temperature. The reaction was found to be in reasonable accord with second-order kinetics. G.p.c. analysis of PC after reaction with the model secondary amine compound in solution at 65°C and in the melt at 270°C also established that the reaction was quantitative. Reduced domain sizes, as seen by TEM, give evidence of chemical compatibilization of melt blended PC/SAN/SAN–amine mixtures. Subsequent papers will report on the morphological development and stability of compatibilized PC/SAN and PC/ABS blends and the mechanical properties of these materials.

Acknowledgements

This research was supported by the US Army Research Office. Various polymers used in this work were kindly supplied by Bayer Corporation, Mitsubishi Engineering Plastics Corporation and The Dow Chemical Company.

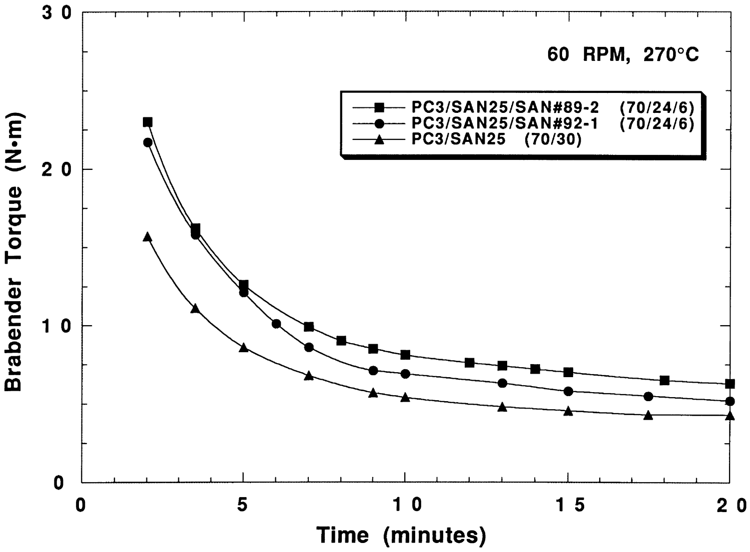

Fig. 13. Brabender torque versus time for the melt blends (270°C at a rotor speed of 60 rev min^{-1}) of VH-PC/SAN25/SAN–amine#2 (70/30–X/X).

References

[1] Grabowski TS. US Pat 3 130 177, 1964 (to Borg-Warner Corp.).
[2] Lantos PR. In: Proc 4th International Congress on Compatibilizers and Reactive Polymer Alloying (Compalloy '91), New Orleans, LA, 1991:41.
[3] Bucknall CB. Toughened plastics. Essex: Applied Science Publishers, 1977.
[4] Utracki LA. Polymer alloys and blends. Munich: Carl Hanser Verlag, 1989.
[5] Favis BD. Can J Chem Eng 1991;69:619.
[6] Lombardo BS, Keskkula H, Paul DR. J Appl Polym Sci 1994;54:1697.
[7] Wu J, Shen S, Chang F. J Appl Polym Sci 1993;50:1379.
[8] Sweeney FM, editor. Polymer blends and alloys: guidebook to commercial products. Lancaster, PA: Technomic Publishing, 1988.
[9] Ishikawa M, Chiba I. Polymer 1990;31:1232.
[10] Greco R. In: Martuscelli E, Musto P, Ragosta G, editors. Advanced routes for polymer toughening. Amsterdam: Elsevier, 1996:Ch. 9.
[11] Mendelson RA. J Polym Sci, Polym Phys Edn 1985;23:1975.
[12] Keitz JD, Barlow JW, Paul DR. J Appl Polym Sci 1984;29:3131.
[13] Cheng TW, Keskkula H, Paul DR. J Appl Polym Sci 1992;45:1245.
[14] Quintens D, Groeninckx G, Guest M, Aerts L. Polym Eng Sci 1990;30:1474.
[15] Callaghan TA, Takakuwa K, Paul DR, Padwa AR. Polymer 1993;34:3796.
[16] Greco R, Sorrentino A. Adv Polym Technol 1994;13:249.
[17] Guest MJ, Daly JH. Eur Polym J 1989;25:985.
[18] Guest MJ, Daly JH. Eur Polym J 1990;26:603.
[19] Kim WN, Burns CM. Polym Eng Sci 1988;28:1115.
[20] Kim CK, Paul DR. Polymer 1992;33:4941.
[21] Kim H, Keskkula H, Paul DR. Polymer 1991;32:1447.
[22] Janarthanan V, Stein RS, Garrett PD. J Polym Sci: Part B: Polym Phys 1993;31:1995.
[23] Quintens D, Groeninckx G, Guest M, Aerts L. Polym Eng Sci 1990;30:1484.
[24] Fortelny I, Zivny A. Polymer 1995;36:4113.
[25] Macosko CW, Guegan P, Khandpur AK, Nakayama A, Marechal P, Inoue T. Macromolecules 1996;29:5590.
[26] Majumdar B, Keskkula H, Paul DR. Polymer 1994;35:1386.
[27] Sondergaard K, Lyngaae-Jorgensen J. In: Nakatani AI, Dadmun MD, editors. Flow-induced structure in polymers. ACS Symposium Series, vol. 597. Washington, DC: American Chemical Society, 1995:Ch. 12.
[28] Sundararaj U, Macosko CW. Macromolecules 1995;28:2647.
[29] Paul DR. In: Paul DR, Newman S, editors. Polymer blends. New York: Academic Press Inc., 1978:Ch. 12.
[30] Chen CC, White JL. SPE ANTEC '91 1991:969.
[31] Chen CC, White JL. Polym Eng Sci 1993;33:923.
[32] Liu NC, Baker WE. Adv Polym Technol 1992;11:249.
[33] Min K, White JL, Fellers JF. Polym Eng Sci 1984;24:1327.
[34] Wu S. Polymer interface and adhesion. New York: Marcel Dekker, 1982.
[35] Okamoto M, Inoue T. Polym Eng Sci 1993;33:175.
[36] Majumdar B, Paul DR, Oshinski AJ. Polymer 1997;38:1787.
[37] Paul DR. In: Paul DR, Newman S, editors. Polymer blends. New York: Academic Press, 1978:Ch. 1.
[38] Xanthos M, Dagli SS. Polym Eng Sci 1991;31:929.
[39] Brown SB. In: Xanthos M, editor. Reactive extrusion principles and practice. Munich: Hanser, 1992:Ch. 4.
[40] Schmitt BJ. Angew Chem Int Ed Engl 1979;18:273.
[41] Padwa AR, Saski Y, Wolske KA, Macosko CW. J Polym Sci: Part A: Polym Chem 1995;33:2165.
[42] Padwa AR, Lavengood RE. Polym Prepr, ACS Div Polym Chem 1992;33 (2):600.
[43] Vermeesch I, Groeninckx G. J Appl Polym Sci 1994;53:1365.
[44] Song Z, Baker WF. J Polym Sci: Part A: Polym Chem 1992;30:1589.
[45] Ide F, Hasegawa A. J Appl Polym Sci 1974;18:963.
[46] Padwa AR. Polym Eng Sci 1992;32:1703.
[47] Hobbs SY, Bopp RC, Watkins VH. Polym Eng Sci 1983;23:380.
[48] Gonzalez-Montiel A, Keskkula H, Paul DR. J Polym Sci: Part B: Polym Phys 1995;33:1751.
[49] Lavengood RE, Silver FM. SPE ANTEC '87 1987;45:1369.
[50] Lavengood RE, Padwa AR, Harris AF. US Pat. 4 713 415, 1987 (to Monsanto).
[51] Majumdar B, Keskkula H, Paul DR, Harvey NG. Polymer 1994;35:4263.
[52] Triacca VJ, Ziaee S, Barlow JW, Keskkula H, Paul DR. Polymer 1991;32:1401.
[53] Liu WB, Chang FC. Polym Prepr, ACS Div Polym Chem 1993;34:803.
[54] Maa CT, Chang FC. J Appl Polym Sci 1993;49:913.
[55] Lee PC, Kuo WF, Chang FC. Polymer 1994;35:5641.
[56] Holsti-Miettinen RM, Heino MT, Seppala JV. J Appl Polym Sci 1995;57:573.

[57] Ito Y, Hiromi O, Yasuyuki I, Ohtani H, Shin T. Polym J 1996;28:1090.

[58] Kirchner K. Kunststoffe 1987;77:993.

[59] Foldi VS, Campbell TW. J Polym Sci 1962;56:1.

[60] Schafer R, Kressler J, Neuber R, Mulhaupt R. Macromolecules 1995;28:5037.

[61] Montaudo G, Puglisi C, Samperi F. J Polym Sci: Part A: Polym Chem 1994;32:15.

[62] Montaudo G, Puglisi C, Samperi F, Lamantia FP. J Polym Sci: Part A: Polym Chem 1996;34:1283.

[63] Gattiglia E, Turturro A, Pedemonte E. J Appl Polym Sci 1989;38:1807.

[64] Gattiglia E, Turturro A, Lamantia FP, Valenza A. J Appl Polym Sci 1992;46:1887.

[65] Tobolsky AV, Yu H, Thach R. J Appl Polym Sci 1962;VI:S44.

[66] Grassie N. In: Brandrup J, Immergut EH, editors. Polymer handbook. New York: Wiley, 1989:Ch. II-380.

[67] Meckel W, Goyert W, Wieder W. In: Legge NR, Holden G, Schroeder HE, editors. Thermoplastic elastomers: a comprehensive review. Munich: Hanser, 1987:Ch. 2.

[68] Fabris HJ. In: Frisch KC, Reegen SL, editors. Advances in urethane science and technology. Stamford, CT: Technomic, 1978:173.

[69] Saunders JH, Frisch KC. Polyurethanes: chemistry and technology II. New York: Interscience Publishers, 1964:388.

[70] Foti S, Giuffrida M, Maravigna P, Montaudo G. J Polym Sci, Polym Chem Edn 1983;21:1599.

[71] Magnusson AB. J Appl Polym Sci 1967;11:2175.

[72] Hu G, Sun Y, Lambla M. Polym Eng Sci 1996;36:676.

[73] Ueda K, Hirao A, Nakahama S. Macromolecules 1990;23:939.

[74] Quirk RP, Cheng P. Macromolecules 1986;19:1291.

[75] Kim YJ, Glass TE, Lyle GD, McGrath JE. Macromolecules 1993;26:1344.

[76] Li M, Ma CM, Lin M, Lu M, Chen J, Chang F. Polymer 1997;38:845.

[77] Sebenik A, Osredkar U, Vizovisek I. J Macromol Sci 1986; A23:369.

[78] Natansohn A, Rutkowska M, Eisenberg A. Polym Eng Sci 1987;27:1504.

[79] Wurm B, Keul H, Hoecker H. Macromolecules 1992;25:2977.

[80] Liu LB, Sumita M, Miyasaka K. Macromolecules 1988;21:3424.

[81] Oshinski AJ, Keskkula H, Paul DR. Polymer 1992;33:268.